

**Manuscript version: Published Version**

The version presented in WRAP is the published version (Version of Record).

**Persistent WRAP URL:**

<http://wrap.warwick.ac.uk/137940>

**How to cite:**

The repository item page linked to above, will contain details on accessing citation guidance from the publisher.

**Copyright and reuse:**

The Warwick Research Archive Portal (WRAP) makes this work by researchers of the University of Warwick available open access under the following conditions.

Copyright © and all moral rights to the version of the paper presented here belong to the individual author(s) and/or other copyright owners. To the extent reasonable and practicable the material made available in WRAP has been checked for eligibility before being made available.

Copies of full items can be used for personal research or study, educational, or not-for-profit purposes without prior permission or charge. Provided that the authors, title and full bibliographic details are credited, a hyperlink and/or URL is given for the original metadata page and the content is not changed in any way.

**Publisher's statement:**

Please refer to the repository item page, publisher's statement section, for further information.

For more information, please contact the WRAP Team at: [wrap@warwick.ac.uk](mailto:wrap@warwick.ac.uk)

# Extremely slow nonequilibrium monopole dynamics in classical spin ice

T. Stöter<sup>1,2</sup>, M. Doerr<sup>1</sup>, S. Granovsky<sup>1,3</sup>, M. Rotter<sup>4</sup>, S. T. B. Goennenwein<sup>1</sup>, S. Zherlitsyn<sup>2</sup>,  
O. A. Petrenko<sup>5</sup>, G. Balakrishnan<sup>5</sup>, H. D. Zhou<sup>6,7</sup> and J. Wosnitzer<sup>1,2</sup>

<sup>1</sup>*Institute for Solid State and Materials Physics and Würzburg-Dresden Cluster of Excellence ct.qmat, TU Dresden, 01062 Dresden, Germany*

<sup>2</sup>*Hochfeld-Magnetlabor Dresden (HLD-EMFL), Helmholtz-Zentrum Dresden-Rossendorf, 01328 Dresden, Germany*

<sup>3</sup>*Faculty of Physics, M. V. Lomonosov Moscow State University, Moscow 119991, Russia*

<sup>4</sup>*McPhase Project, 01159 Dresden, Germany*

<sup>5</sup>*Department of Physics, University of Warwick, Coventry CV4 7AL, United Kingdom*

<sup>6</sup>*Department of Physics and Astronomy, University of Tennessee, Knoxville, Tennessee 37996-1200, USA*

<sup>7</sup>*National High Magnetic Field Laboratory, Florida State University, Tallahassee, Florida 32306-4005, USA*



(Received 5 February 2020; revised manuscript received 13 May 2020; accepted 26 May 2020; published 11 June 2020)

We report on the nonequilibrium monopole dynamics in the classical spin ice  $\text{Dy}_2\text{Ti}_2\text{O}_7$  detected by means of high-resolution magnetostriction measurements. Significant lattice changes occur at the transition from the kagome-ice to the saturated-ice phase, visible in the longitudinal and transverse magnetostriction. A hysteresis opening at temperatures below 0.6 K suggests a first-order transition between the kagome and saturated state. Extremely slow lattice relaxations, triggered by changes of the magnetic field, were observed. These lattice-relaxation effects result from nonequilibrium monopole formation or annihilation processes. The relaxation times extracted from our experiment are in good agreement with theoretical predictions with decay constants of the order of  $10^4$  s at 0.3 K.

DOI: [10.1103/PhysRevB.101.224416](https://doi.org/10.1103/PhysRevB.101.224416)

## I. INTRODUCTION

Magnetically frustrated materials are the subject of intense research due to inherently competing interactions, large ground-state degeneracy, the appearance of exotic states, such as spin-ice and spin-liquid phases [1,2], deconfined fractionalized excitations (magnetic monopoles) [3], nonstationary processes [4–6], and unusual spin dynamics [7–13]. However, an analysis of the long-term nonequilibrium processes at low fields has not been sufficiently elaborated; cf. [11].

Prominent examples of frustrated magnetic systems are the pyrochlore oxides  $\text{A}_2\text{B}_2\text{O}_7$ , with a trivalent rare-earth ion  $\text{A}^{3+}$  and a tetravalent ion  $\text{B}^{4+}$ . Especially in the pyrochlores with Dy or Ho on the A site, many different exotic states have been revealed. The single-ion ground state can be treated as an effective spin-half state [14]. The two-ion interaction is very well described by the dipolar spin-ice model [15], which includes dipolar and exchange interactions that result in an effective ferromagnetic nearest-neighbor interaction. These interactions, together with strong magnetic anisotropy due to crystal-electric-field (CEF) effects, favor the highly degenerate spin-ice configuration: two spins point into and two spins point out of each tetrahedron (“2-in-2-out”) [16]. The excitations of this arrangement to “3-in-1-out” or “1-in-3-out” can be interpreted as the creation of magnetic monopole-antimonopole pairs [3].

The study of thermally activated spin dynamics in  $\text{Dy}_2\text{Ti}_2\text{O}_7$  via ac susceptibility or magnetization is the focus of numerous publications [12,17–26] because these slow dynamic effects are directly connected to the kinetics and interactions of these monopoles. In detail, a sharp increase

of the relaxation times at temperatures below 1 K was reported and attributed to the Coulomb-gas character of charged particles (monopoles) forming a network of “Dirac strings.” This blocks the monopoles in metastable states [27–29]. The temperature-dependent nonequilibrium dynamics was analyzed theoretically in Ref. [30]. Field-dependent magnetic investigations which also resolve the monopole dynamics in the kagome-ice state or in the saturated spin ice in relation to the crystal lattice are, although of great interest [31], rather rare and, therefore, are the main topic of this paper.

Several theoretical [32–41] and experimental studies [5,6,42] have investigated the magnetoelastic coupling in pyrochlore systems. As frustration is highly dependent on the symmetry of the lattice, distorting the lattice can relieve the frustration. The spin-ice state was shown to be stable under hydrostatic pressure [42]. Likewise lifting the degeneracy of the frustrated state by a magnetic field could also influence the lattice.

In ultrasound measurements on  $\text{Dy}_2\text{Ti}_2\text{O}_7$ , dramatic nonequilibrium effects were found: thermal runaway associated with monopole avalanches [5]. In the magnetization, these kinds of avalanches also exist [43]. Apart from these short-time-scale effects, an increase of the time scale of the internal dynamics has been observed in various measurements on spin ice, such as in ac susceptibility [12,17–24,26,44], magnetization [11,20,43], the magnetocaloric effect [45], thermal conductivity [46], and heat capacity [47]. Most of these measurements were performed quenching the sample from low fields to zero. From theory, another kind of nonequilibrium effect when quenching the field from the monopole-rich saturated-ice or kagome-ice phase towards the

spin-ice phase with only a few monopoles was suggested. Both short- and long-time annihilation processes have been proposed in the theory work of Mostame *et al.* [31]. In experiment, a slow relaxation process has been reported to occur [11]. These investigations, however, were performed only at very low magnetic fields. In our studies, on the other hand, we investigate in detail nonequilibrium processes at higher fields, in the kagome-ice state, and, thereby, validate the theoretically proposed slow dynamics due to a dynamical arrest owing to the appearance of field-induced energy barriers to monopole motion [31].

In detail, we observed extremely slow lattice-relaxation processes which can be directly connected to the generation and annihilation of monopole/antimonopole pairs in magnetic field. These macroscopic lattice changes allow us a direct insight into the microscopic spin dynamics. Via magnetoelastic coupling we can indirectly resolve the relevant minute magnetization changes with extraordinarily high resolution.

## II. EXPERIMENTAL

Single crystals of  $\text{Dy}_2\text{Ti}_2\text{O}_7$  were grown by the floating-zone technique [48] and oriented along the required crystallographic axes using x-ray Laue diffraction. On the role of disorder, data obtained at these single crystals were published in [10,25]. The crystals used for the experiments were oblate cuboids of dimensions  $\sim 3 \times 2 \times 1 \text{ mm}^3$ , for which a demagnetization factor of about 0.7 for fields along the shortest dimension was deduced.

For the measurements, we used a capacitive dilatometer [49] that was mounted on a probe placed in a sorb-pumped  $^3\text{He}$  cryostat reaching temperatures down to 0.3 K. The estimated magnetic-field misorientation is less than  $\pm 3^\circ$ .

For accurate monitoring and control of the dilatometer and sample temperature we used a Cernox and a  $\text{RuO}_2$  thermometer (below 1 K). Both thermometers were attached to the dilatometer cell close to the sample. The temperature stability is of crucial importance, since in earlier experiments [5,11,43] magnetothermal avalanches ramping down the field to zero and an increase of sample temperature by field sweeps were observed. In our experiment we found an increase of the temperature by 10 mK during the field sweeps. After 300 s waiting time, the temperature had completely stabilized.

## III. RESULTS

First, we focus on the (static) low-temperature magnetostriction curves displayed in Fig. 1. Sweeping the field up at lowest temperature of 0.3 K in longitudinal geometry, the crystal contracts at first until it reaches a minimum at around 0.8 T, then expands up to about 1.3 T. Upon further increasing the field, it contracts again reaching a local minimum and turning again to expand linearly with increasing field with a slope of about  $1 \times 10^{-5} \text{ T}^{-1}$ . Sweeping further up in field, there is no sign of saturation up to 10 T (not shown). Our mean-field calculations using a model described in [50] and the software package MCFHASE [51] show [Fig. 1(c)] that the longitudinal magnetostriction changes are caused by exchange striction and CEF striction effects stemming from mixing in the higher CEF terms. Note that the relaxation

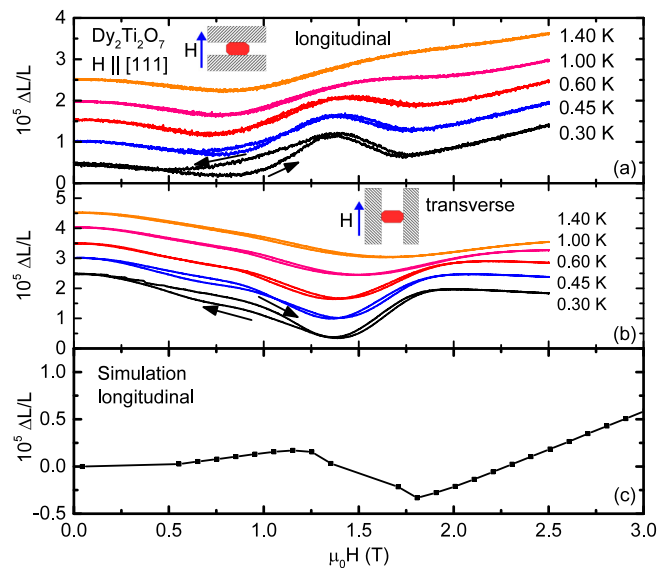


FIG. 1. Field dependence of the relative sample-length change parallel and perpendicular to a magnetic field applied along the [111] direction at various temperatures: (a) longitudinal magnetostriction; (b) transversal magnetostriction. The curves are offset for clarity. (c) Model calculation of longitudinal magnetostriction at 0.3 K.

processes due to monopole dynamics discussed below are dominated by exchange striction effects. The magnetostriction in transversal geometry is of roughly the opposite character. All magnetostrictive effects are on the order of  $10^{-5}$ , well above the noise level of about  $10^{-7}$ . There is a distinct anomaly at about 1.3 T. The following decrease/increase of the sample length is magnetically caused by exchange. (Note: the experimental data are related to the external field; the internal field is lower; see below.) It corresponds to the first-order transition between the kagome and “3-in-1-out” state [52] in good agreement with our own simulations. In the following, we will only discuss the results obtained in longitudinal geometry. The transverse magnetostriction shows similar relaxation phenomena as discussed below.

In the kagome-ice region, we observe a clear hysteresis below 0.6 K (Fig. 1). It must be assumed that extensive dynamic effects are present in this area and that the sample is not in an equilibrium state in this range.

Some typical relaxation data for  $\text{Dy}_2\text{Ti}_2\text{O}_7$  in longitudinal geometry are shown in Fig. 2 for various temperatures. These plots display the changes in sample length as a function of time: Fig. 2(a) shows the data after rapid (1 T/min) reduction of the magnetic field and Fig. 2(b) those after field increase. While decreasing the field [Fig. 2(a)], the lattice contracts quickly, but even after we stop the field sweep, the lattice still continues to contract very slowly. For 0.3 and 0.45 K, even after 1 h no steady state is reached. At 0.6 K, the lattice changes stop after about 600 s, i.e., the lattice relaxation is slower at lower temperatures. We found corresponding behavior for increasing fields [Fig. 2(b)]. During the sweeps, the lattice expands quickly and continues to do so very slowly even after stopping the sweep. Again, we observe much longer time scales of the lattice relaxation the lower the temperature.

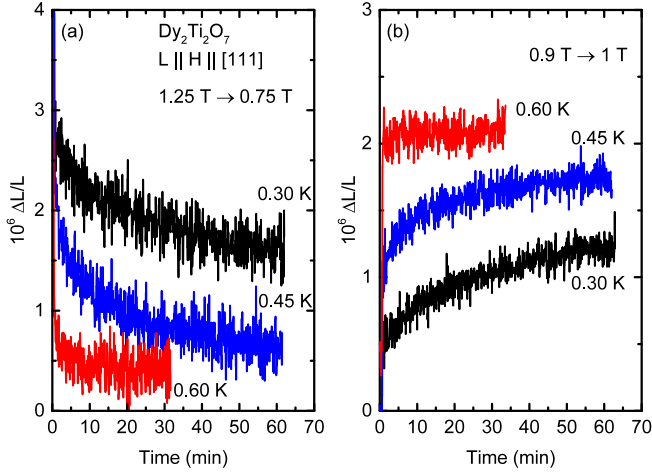


FIG. 2. Typical time dependence of the relative sample length of  $\text{Dy}_2\text{Ti}_2\text{O}_7$  in longitudinal geometry  $H \parallel \Delta L/L$  at various temperatures (a) sweeping the field quickly from 1.25 down to 0.75 T and (b) sweeping from 0.90 up to 1.00 T.

#### IV. ANALYSIS AND DISCUSSION

In order to analyze the data quantitatively and to obtain more insight into the nonequilibrium dynamics involved, we need some model to describe the relaxation time. It seems reasonable that some exponential decay law should be adequate to describe the data, but the exact form is not *a priori* known. Therefore, we performed a long-time relaxation measurement (10 h, Fig. 3) to better resolve the decay law. The field was swept from 1.25 to 0.75 T at 0.3 K.

Possible models would be a simple exponential decay with one relaxation time

$$(\Delta L/L)(t) = (\Delta L/L)_\infty + A e^{-(t-t_0)/\tau}, \quad (1)$$

or a stretched-exponential decay

$$(\Delta L/L)(t) = (\Delta L/L)_\infty + A e^{-[(t-t_0)/\tau]^\beta}, \quad (2)$$

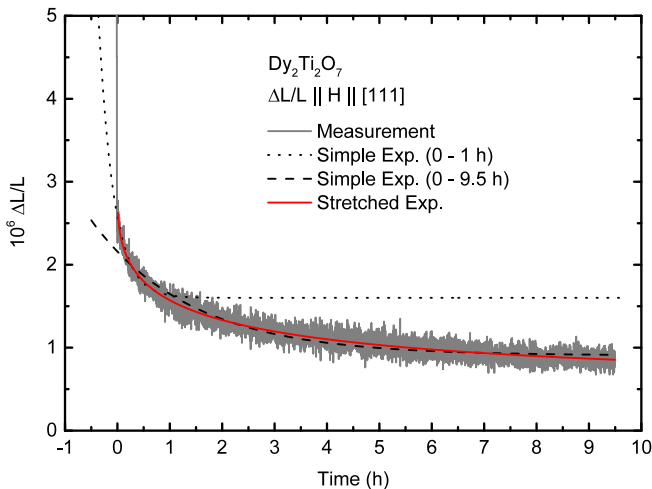


FIG. 3. Long-time change of the sample length after a quick field sweep from 1.25 to 0.75 T and fit lines using different models to describe the data.

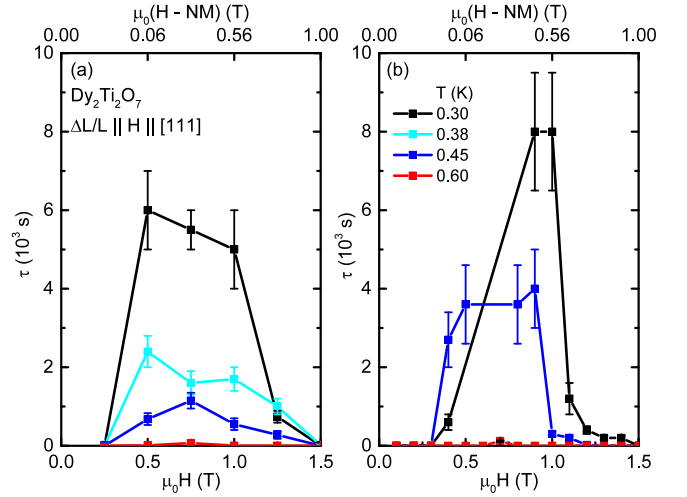


FIG. 4. Field dependence of the relaxation times of  $\text{Dy}_2\text{Ti}_2\text{O}_7$  at various magnetic fields in longitudinal geometry  $H \parallel \Delta L/L$  after (a) reducing and (b) increasing the magnetic field quickly with 1 T/min. The final external field is shown on the bottom axis. The initial field was always (a) 0.5 T higher and (b) 0.1 T lower than the final field. The internal field after demagnetization correction is labeled on the top axis for the external fields 0.5, 1.0, and 1.5 T.

where  $\tau$  is the relaxation time,  $\beta$  an exponent describing the relaxation-time distribution,  $(\Delta L/L)_\infty$  the relative sample-length change for  $t \rightarrow \infty$ , and  $(\Delta L/L)_\infty + A$  gives the value of  $(\Delta L/L)$  at  $t = t_0$ , with  $t_0$  usually set to zero. The data were described using the free parameters  $A$ ,  $(\Delta L/L)_\infty$ , and  $\tau$  for both equations and additionally  $\beta$  for the stretched-exponential fit. We found that simple exponential decays using Eq. (1) deviate significantly from the data, either at the beginning or at the end of the relaxation process (dashed and dotted lines in Fig. 3, respectively). On the other hand, the stretched exponential fit provides a much better match to the data in the whole time range (red line in Fig. 3). The stretched-exponential model describes the data best for  $\beta = 0.4$  and  $\tau = 5500$  s.

A model with two relaxation times  $\tau_S$  and  $\tau_L$  to distinguish between free and bound monopoles, as proposed in [20], describes our data less well, although even more parameters are used. Indeed, the stretched-exponential model is better motivated: first, we observed that any exponential-decay fit saturates too early and should be stretched over longer times. Secondly, applying the model [Eq. (2)] is justified by the existence of the mutual interactions of the magnetic monopoles as suggested by theoretical investigations of the spin-ice model [31,53]. Indeed, this model leads to a distribution of relaxation times. In particular, the formation of incontractable monopole-antimonopole pairs might lead to a slowing down of the dynamics.

In the following, we fixed  $\beta$  to 0.4 and used Eq. (2) to describe our lattice-relaxation data (such as those shown in Fig. 2). The error bars were estimated by varying  $\beta$  by  $\pm 0.2$  and checking whether the data could be described with another set of  $A$  and  $\tau$ .

Figure 4 shows the field dependence of the extracted relaxation times of  $\text{Dy}_2\text{Ti}_2\text{O}_7$  after rapidly decreasing [Fig. 4(a)]



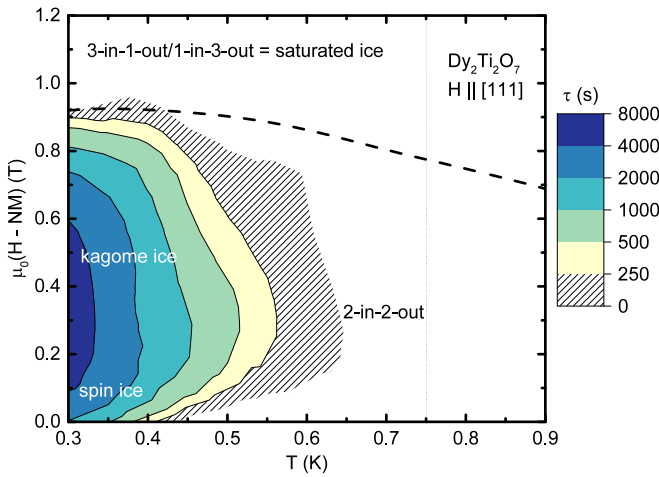


FIG. 5. Contour plot of the relaxation time of  $\text{Dy}_2\text{Ti}_2\text{O}_7$  in the phase space of temperature and internal field with long relaxation times in blue and short relaxation fading to lighter colors. The relaxation times are taken from the quench experiments summarized in Fig. 4. Note the exponential scale of the color code. For comparison, transitions extracted from specific-heat and magnetization data [52] are included as a dashed line.

and increasing the field [Fig. 4(b)]. The longest relaxation times were measured in the field region between 0.5 and 1.0 T. Nonequilibrium dynamics could not be observed at fields below 0.2 T or above 1.3 T. The time scales of the relaxation are up to hours at 0.3 K and a few minutes at 0.6 K. Above 0.7 K, no relaxation could be found. This matches approximately the spin-freezing temperature of about 0.6 K [54]. The extremely slow spin dynamics, therefore, is only present in the kagome-ice region below the saturated-ice phase [52,55].

Finally, we summarize the relaxation times of our field-quench experiments in a phase diagram of temperature and internal field (corrected for demagnetization effects) in Fig. 5. The internal field is calculated using  $B_{\text{int}} = \mu_0(H - NM)$ , where  $\mu_0 H$  is the applied field,  $N$  the demagnetizing factor, and  $M$  the known magnetization [56]. In accordance with the known phase diagram of  $\text{Dy}_2\text{Ti}_2\text{O}_7$  extracted from specific-heat and magnetization data [52], the lattice relaxation is only observed below the transition from the kagome-ice to saturated-ice phase (dashed line in Fig. 5). The temperature-dependent relaxation time decreases with increasing temperature. The longest relaxation times are found in the kagome-ice phase at low temperatures. The region of our measurable times (minimum 30 s) extends to 0.6 K, the spin-freezing temperature [19]. At higher temperatures the relaxations could no longer be resolved.

To discuss the experimental facts, the field-quench experiments make the dynamics of thermally activated monopoles in the kagome phase of spin-ice compounds experimentally accessible. The magnetostriction is a highly sensitive probe to study the monopole dynamics, specifically in the kagome-ice state. Our investigations on  $\text{Dy}_2\text{Ti}_2\text{O}_7$  evidence the dynamical behavior in spin ice as it has been modeled in theory with monopole “3-in-1-out” or “1-in-3-out” excitations

from the ground-state configuration of “2-in-2-out” [30,31]. In particular, a significant increase of the time scales of these dynamics at temperatures below 0.6 K has been found. A number of publications deal with the spin dynamics of pyrochlore compounds, specifically in  $\text{Dy}_2\text{Ti}_2\text{O}_7$  [20,31,43]. Dynamical effects apparently of the same origin though with a somewhat different time scale below 1 K were observed in magnetization and magnetic ac susceptibility ( $10^5$  s at 0.3 K in [20,43]), and predicted from theory [31] as well. The relaxation is strongly temperature dependent, especially in the range between 0.3 and 0.5 K, so that deviations in the absolute values can be expected. However, the strong increase of the relaxation time to low temperatures is characteristic for all data.

Many earlier investigations show dynamic effects below 1 K on the same order of magnitude as the lattice relaxation and probably having the same origin. Our results confirm that the crystal lattice is active in the magnetic relaxation processes and directly reflects this relaxation. One would expect different relaxation times for rising and falling magnetic fields. According to [31], the formation of monopole-antimonopole pairs in increasing fields should lead to a shorter time constant, whereas the annihilation of monopole-antimonopole pairs in decreasing field is a slower process due to rearranging of dimers. Remarkably, within experimental error, the observed relaxation times for decreasing and increasing field are of the same order of magnitude. Pinning effects at impurities [57], which could slow down the free movement of monopoles during the creation process, are a possible reason for this behavior. This issue needs further investigations. Our measurements also show an increase of the relaxation times especially in the kagome-ice phase where we could follow the monopole dynamics over long time periods. This is in reasonable qualitative agreement with theoretical predictions [31]. The microscopic picture is that monopole-antimonopole pairs (“3-in-1-out” or vice-versa configurations) on neighboring tetrahedra form stable bound pairs, that can neither annihilate nor move away from each other due to their mutual interaction. Therefore, the monopole mobility or spin-flip rate is reduced. Consequently, the probability of the annihilation of monopoles is suppressed and it takes a long time for this process to happen. The monopole movement (spin flips) might be suppressed at defect sites of the lattice slowing down the intrinsic dynamics [57]; this was suggested to explain the difference between the long-time thermal relaxation in specific-heat measurements [47] in comparison to other experiments [13,58].

## V. SUMMARY

In summary, we have shown dilatometric results of the lattice relaxation due to monopole dynamics in the classical spin ice compound  $\text{Dy}_2\text{Ti}_2\text{O}_7$ . The lattice relaxation follows a stretched-exponential law with temperature- and field-dependent relaxation times  $\tau$ . The analyzed field dependence of the relaxation, presented here using magnetostriction, illustrates the different character of the individual states. Extremely long relaxation times were observed in the kagome ice. Our results fit well to the behavior expected from theoretical considerations.

We acknowledge support from HLD at HZDR, member of the European Magnetic Field Laboratory (EMFL). This research has been supported by the DFG through SFB 1143 (Project-ID No. 247310070) and the excellence cluster EXC2147 “ct.qmat” (Project-ID No. 390858490). The work

at the University of Warwick was supported by a grant from the EPSRC, UK (No. EP/M028771/1). A portion of this work was performed at the NHMFL, which is supported by the NSF Cooperative Agreement No. DMR-1644779 and the State of Florida.

- [1] R. Moessner and A. Ramirez, *Phys. Today* **59**(2), 24 (2006).
- [2] L. Balents, *Nature (London)* **464**, 199 (2010).
- [3] C. Castelnovo, R. Moessner, and S. L. Sondhi, *Nature (London)* **451**, 42 (2008).
- [4] D. Slobinsky, C. Castelnovo, R. A. Borzi, A. S. Gibbs, A. P. Mackenzie, R. Moessner, and S. A. Grigera, *Phys. Rev. Lett.* **105**, 267205 (2010).
- [5] S. Erfanifam, S. Zherlitsyn, J. Wosnitzer, R. Moessner, O. A. Petrenko, G. Balakrishnan, and A. A. Zvyagin, *Phys. Rev. B* **84**, 220404(R) (2011).
- [6] S. Erfanifam, S. Zherlitsyn, S. Yasin, Y. Skourski, J. Wosnitzer, A. A. Zvyagin, P. McClarty, R. Moessner, G. Balakrishnan, and O. A. Petrenko, *Phys. Rev. B* **90**, 064409 (2014).
- [7] R. Borzi, F. Gomez Albarracin, H. Rosales, G. Rossini, A. Steppke, D. Prabhakaran, A. Mackenzie, D. Cabra, and S. Grigera, *Nat. Commun.* **7**, 12592 (2016).
- [8] V. Kaiser, S. T. Bramwell, P. C. W. Holdsworth, and R. Moessner, *Phys. Rev. Lett.* **115**, 037201 (2015).
- [9] C. Paulsen, S. Giblin, E. Lhotel, D. Prabhakaran, K. Matsuhira, G. Balakrishnan, and S. Bramwell, *Nat. Commun.* **10**, 1509 (2019).
- [10] C. Paulsen, S. Giblin, E. Lhotel, B. Canals, D. Prabhakaran, K. Matsuhira, and S. Bramwell, *Nat. Phys.* **12**, 661 (2016).
- [11] C. Paulsen, M. J. Jackson, E. Lhotel, B. Canals, D. Prabhakaran, K. Matsuhira, S. R. Giblin, and S. T. Bramwell, *Nat. Phys.* **10**, 135 (2014).
- [12] L. R. Yaraskavitch, H. M. Revell, S. Meng, K. A. Ross, H. M. L. Noad, H. A. Dabkowska, B. D. Gaulin, and J. B. Kycia, *Phys. Rev. B* **85**, 020410(R) (2012).
- [13] S. R. Giblin, M. Twengström, L. Bovo, M. Ruminy, M. Bartkowiak, P. Manuel, J. C. Andresen, D. Prabhakaran, G. Balakrishnan, E. Pomjakushina, C. Paulsen, E. Lhotel, L. Keller, M. Frontzek, S. C. Capelli, O. Zaharko, P. A. McClarty, S. T. Bramwell, P. Henelius, and T. Fennell, *Phys. Rev. Lett.* **121**, 067202 (2018).
- [14] J. G. Rau and M. J. P. Gingras, *Phys. Rev. B* **92**, 144417 (2015).
- [15] B. C. den Hertog and M. J. P. Gingras, *Phys. Rev. Lett.* **84**, 3430 (2000).
- [16] S. T. Bramwell, *Science* **294**, 1495 (2001).
- [17] K. Matsuhira, Y. Hinatsu, and T. Sakakibara, *J. Phys.: Condens. Matter* **13**, L737 (2001).
- [18] J. Snyder, B. G. Ueland, J. S. Slusky, H. Karunadasa, R. J. Cava, A. Mizel, and P. Schiffer, *Phys. Rev. Lett.* **91**, 107201 (2003).
- [19] J. Snyder, B. G. Ueland, J. S. Slusky, H. Karunadasa, R. J. Cava, and P. Schiffer, *Phys. Rev. B* **69**, 064414 (2004).
- [20] K. Matsuhira, C. Paulsen, E. Lhotel, C. Sekine, Z. Hiroi, and S. Takagi, *J. Phys. Soc. Jpn.* **80**, 123711 (2011).
- [21] K. Matsuhira, Y. Hinatsu, K. Tenya, and T. Sakakibara, *J. Phys.: Condens. Matter* **12**, L649 (2000).
- [22] J. Snyder, J. S. Slusky, R. J. Cava, and P. Schiffer, *Nature (London)* **413**, 48 (2001).
- [23] G. Ehlers, A. L. Cornelius, M. Orendá, M. Kajnakov, T. Fennell, S. T. Bramwell, and J. S. Gardner, *J. Phys.: Condens. Matter* **15**, L9 (2003).
- [24] G. Ehlers, A. L. Cornelius, T. Fennell, M. Koza, S. T. Bramwell, and J. S. Gardner, *J. Phys.: Condens. Matter* **16**, S635 (2004).
- [25] O. A. Petrenko, M. R. Lees, and G. Balakrishnan, *J. Phys.: Condens. Matter* **23**, 164218 (2011).
- [26] J. A. Quilliam, L. R. Yaraskavitch, H. A. Dabkowska, B. D. Gaulin, and J. B. Kycia, *Phys. Rev. B* **83**, 094424 (2011).
- [27] L. C. Jaubert and P. C. W. Holdsworth, *Nat. Phys.* **5**, 258 (2009).
- [28] L. C. Jaubert and P. C. W. Holdsworth, *J. Phys.: Condens. Matter* **23**, 164222 (2011).
- [29] S. R. Giblin, S. T. Bramwell, P. C. W. Holdsworth, D. Prabhakaran, and I. Terry, *Nat. Phys.* **7**, 252 (2011).
- [30] C. Castelnovo, R. Moessner, and S. L. Sondhi, *Phys. Rev. Lett.* **104**, 107201 (2010).
- [31] S. Mostame, C. Castelnovo, R. Moessner, and S. L. Sondhi, *Proc. Natl. Acad. Sci. USA* **111**, 640 (2014).
- [32] Y. Yamashita and K. Ueda, *Phys. Rev. Lett.* **85**, 4960 (2000).
- [33] O. Tchernyshyov, R. Moessner, and S. L. Sondhi, *Phys. Rev. Lett.* **88**, 067203 (2002).
- [34] O. Tchernyshyov, R. Moessner, and S. L. Sondhi, *Phys. Rev. B* **66**, 064403 (2002).
- [35] J. Richter, O. Derzhko, and J. Schulenburg, *Phys. Rev. Lett.* **93**, 107206 (2004).
- [36] C. Jia, J. H. Nam, J. S. Kim, and J. H. Han, *Phys. Rev. B* **71**, 212406 (2005).
- [37] K. Penc, N. Shannon, Y. Motome, and H. Shiba, *J. Phys.: Condens. Matter* **19**, 145267 (2007).
- [38] K. Terao and I. Honda, *J. Phys.: Condens. Matter* **19**, 145261 (2007).
- [39] T. E. Saunders and J. T. Chalker, *Phys. Rev. B* **77**, 214438 (2008).
- [40] S. H. Curnoe, *Phys. Rev. B* **78**, 094418 (2008).
- [41] K. Aoyama and H. Kawamura, *Phys. Rev. Lett.* **116**, 257201 (2016).
- [42] I. Mirebeau and I. Goncharenko, *J. Phys.: Condens. Matter* **16**, S653 (2004).
- [43] M. J. Jackson, E. Lhotel, S. R. Giblin, S. T. Bramwell, D. Prabhakaran, K. Matsuhira, Z. Hiroi, Q. Yu, and C. Paulsen, *Phys. Rev. B* **90**, 064427 (2014).
- [44] H. Takatsu, K. Goto, H. Otsuka, R. Higashinaka, K. Matsubayashi, Y. Uwatoko, and H. Kadowaki, *J. Phys. Soc. Jpn.* **82**, 104710 (2013).
- [45] M. Orendáč, J. Hanko, E. Čížmár, A. Orendáčová, M. Shirai, and S. T. Bramwell, *Phys. Rev. B* **75**, 104425 (2007).
- [46] S. J. Li, Z. Y. Zhao, C. Fan, B. Tong, F. B. Zhang, J. Shi, J. C. Wu, X. G. Liu, H. D. Zhou, X. Zhao, and X. F. Sun, *Phys. Rev. B* **92**, 094408 (2015).

- [47] D. Pomaranski, L. R. Yaraskavitch, S. Meng, K. A. Ross, H. M. L. Noad, H. A. Dabkowska, B. D. Gaulin, and J. B. Kycia, *Nat. Phys.* **9**, 353 (2013).
- [48] G. Balakrishnan, O. A. Petrenko, M. R. Lees, and D. M. Paul, *J. Phys.: Condens. Matter* **10**, L723 (1998).
- [49] R. Küchler, T. Bauer, M. Brando, and F. Steglich, *Rev. Sci. Instrum.* **83**, 095102 (2012).
- [50] M. Doerr, M. Rotter, and A. Lindbaum, *Adv. Phys.* **54**, 1 (2005).
- [51] M. Rotter, D. M. Le, J. Keller, L. G. Pascut, T. Hoffmann, M. Doerr, R. Schedler, P. Fabi, S. Rotter, and M. Banks, McPhase software suite, [www.mcphase.de](http://www.mcphase.de), 2020.
- [52] Z. Hiroi, K. Matsuhira, S. Takagi, T. Tayama, and T. Sakakibara, *J. Phys. Soc. Jpn.* **72**, 411 (2003).
- [53] H. M. Revell, L. R. Yaraskavitch, J. D. Mason, K. A. Ross, H. M. L. Noad, H. A. Dabkowska, B. D. Gaulin, P. Henelius, and J. B. Kycia, *Nat. Phys.* **9**, 34 (2013).
- [54] H. Fukazawa, R. G. Melko, R. Higashinaka, Y. Maeno, and M. J. P. Gingras, *Phys. Rev. B* **65**, 054410 (2002).
- [55] R. Higashinaka, H. Fukazawa, K. Deguchi, and Y. Maeno, *J. Phys.: Condens. Matter* **16**, S679 (2004).
- [56] T. Sakakibara, T. Tayama, Z. Hiroi, K. Matsuhira, and S. Takagi, *Phys. Rev. Lett.* **90**, 207205 (2003).
- [57] J. A. Bloxsom, Ph.D. thesis, University College London, London, 2016.
- [58] P. Henelius, T. Lin, M. Enjalran, Z. Hao, J. G. Rau, J. Altosaar, F. Flicker, T. Yavors'kii, and M. J. P. Gingras, *Phys. Rev. B* **93**, 024402 (2016).